

Copyright

by

Pearl Achuoboro Abue

2021

**The Thesis Committee for Pearl Achuoboro Abue
Certifies that this is the approved version of the following Thesis:**

**EFFICIENCY OF PHOTOCATALYTIC OXIDATION AIR
PURIFIERS IN REMOVING SINGLE AND MULTI-COMPONENT
VOLATILE ORGANIC COMPOUNDS AND DISINFECTION
BYPRODUCTS FROM INDOOR ENVIRONMENTS**

**APPROVED BY
SUPERVISING COMMITTEE:**

Lea Hildebrandt Ruiz, Supervisor

Pawel Misztal

**EFFICIENCY OF PHOTOCATALYTIC OXIDATION AIR
PURIFIERS IN REMOVING SINGLE AND MULTI-COMPONENT
VOLATILE ORGANIC COMPOUNDS AND DISINFECTION
BYPRODUCTS FROM INDOOR ENVIRONMENTS**

by

Pearl Achuoboro Abue

Thesis

Presented to the Faculty of the Graduate School of
The University of Texas at Austin
in Partial Fulfillment
of the Requirements
for the Degree of

Master of Science in Engineering

The University of Texas at Austin

May 2021

Dedication

To my family and friends

Acknowledgements

My deepest appreciation is to my committee. To my supervisor, Professor Lea Hildebrandt Ruiz and to Professor Pawel Misztal for their patience, valuable advice, unending guidance, profound belief in my abilities, and encouragement through this project and while writing my thesis.

I would also like to extend my deepest gratitude to the entire Diatomix filter project team; Professor Lea Hildebrandt Ruiz, Professor Atila Novoselac, Professor Pawel Misztal for their support; Nirvan Bhattacharyya and Mengjia Tang for their guidance and assistance in setting up and running the experiments and with analyzing the data. Many thanks to The National Science Foundation (NSF) for sponsoring this work under project number 1927040 and to our colleagues at The Diatomix Corporation for providing the photocatalytic filters and the air purifier unit used for this project.

Thanks also to the disinfection byproducts team; Professor Lea Hildebrandt Ruiz, Professor Pawel Misztal, Professor Atila Novoselac, Professor Richard Corsi, Professor David Allen for their guidance and mentorship; Nirvan Bhattacharyya, Mengjia Tang, Daniel Blomdahl and Leif Jahn for their contribution in setting up and running the experiments simultaneously with the filter experiments, collecting the data, and for help in collaboratively processing the data.

I am grateful to the Delhi Aerosol Supersite Study team; Professor Lea Hildebrandt Ruiz and Professor Joshua Apte for their guidance; Nisar Baig for consistently running the instruments and collecting data at the Indian Institute of Technology, Delhi; Dr. Sahil Bhandari and Kanan Patel for their knowledge and assistance with processing the data.

Members of the Atmospheric and Physicochemical Processes Group have been an amazing team. Thanks to Nirvan Bhattacharyya for help with setting up and running the experiments, Kanan Patel for taking numerous meetings and responding to my incessant questions while working on the Delhi Aerosol Supersite Study, and to Catherine Masoud, Mrinali Modi, Kristi McPherson, Dr. Sahil Bhandari and Dr. Felipe Cardoso for being great information and learning resources, and great friends.

To my mother and father for all their sacrifice, support, love and prayers and finally to God for seeing me through this journey, I am sincerely grateful.

Abstract

Efficiency of Photocatalytic Oxidation Air Purifiers in Removing Single and Multi-Component Volatile Organic Compounds and Disinfection Byproducts from Indoor Air Environments

Pearl Achuoboro Abue, M.S.E

The University of Texas at Austin, 2021

Supervisor: Lea Hildebrandt Ruiz

The efficiency of a photocatalytic oxidation filter in removing single volatile organic compounds (VOCs) and a mixture of VOCs and disinfection byproducts was studied and compared to that of an activated carbon filter. The filters were set up in a modified portable Bissell400 air purifier unit and deployed in environmental chambers. Results from these experiments suggested that photocatalytic filters may operate more efficiently at higher ultraviolet light wavelengths of 400 nm. They also showed that the efficiency of photocatalytic filters exhibits some compound dependency with methyl ethyl ketone having an efficiency of 3% and 8%, α -pinene having a removal efficiency of 14% and 12 % and Butyric acid having a removal efficiency of 37%. Filtration efficiencies are also impacted by air exchange rates, with higher air exchange rates yielding lower filter efficiencies, and by VOC concentrations, with lower concentrations yielding higher filter efficiencies. Time dependent changes in filter efficiency are also explored briefly and suggest that filter efficiencies decrease over time.

Table of Contents

List of Tables	x
List of Figures	xi
Chapter 1: Introduction	1
Chapter 2: Background	4
2.1 Indoor Air Quality	4
2.2 Cleaning Indoor Air	5
2.2.1 Adsorption.....	6
2.2.2 Photocatalytic Oxidation.....	7
2.2.3 Adsorption and photocatalysis.....	8
2.3 Photocatalytic Oxidation Air Purifiers	9
2.3.1 Parameters influencing photocatalytic oxidation.....	11
2.3.2 Existing Filters	12
2.4 Scope of this Work	12
Chapter 3: Materials and Methods.....	14
3.1 Decay Testing	14
3.2 Instrumentation	15
3.3 Experimental Set Up.....	17
3.4 Data analysis	18
Chapter 4: Results and Discussion.....	22
4.1 Photocatalytic Oxidation and Activated Carbon Efficiencies	22
4.2 Compound Specific Removal Efficiencies for the Photocatalytic Filter.....	23
4.3 Compound Specific Removal Efficiencies for the Activated carbon – Photocatalytic oxidation Hybrid Filter	24

4.4	Uncertainties Related to Experimental Set Up and Low Efficiency Filtration...	26
4.5	Combined Filter Non-Linearity	27
4.6	Filter Efficiency Dependence on Flow Rate, Compound Concentration and Wavelength	30
4.7	Offgassed Compounds From Filter Unit and Filter Media.....	32
Chapter 5: Conclusions and Recommendations		34
5.1	Conclusions.....	34
5.2	Recommendations for Future Work	35
Chapter 6: Summary of Other Works		37
6.1	Observing Seasonal Air Quality Variations from the Delhi Aerosol Supersite (DAS) Study in 2020	37
6.1.1	Materials and Methods.....	37
6.1.2	Overview of seasonal variations in 2020	38
6.1.3	Diurnal variations across the seasons	41
6.1.3	Conclusions and future work	41
Appendix.....		43
References.....		45

List of Tables

Table 3.1: List of experimental conditions for phase 1 decay testing	16
Table 3.2: List of experimental conditions for phase 2 decay testing	17
Table 3.3: Volumetric flowrate, Q_f , through the filter	20
Table 4.1: Comparison of activated carbon and photocatalytic filter efficiencies from phase 1 experiments	22
Table 4.2: Filter efficiencies of 400nm photocatalytic filter	24
Table 4.3: Activated carbon and 400nm photocatalytic filter efficiencies for VOC mixture	25
Table 4.4: Comparison of Phase one and Phase two 400 nm photocatalytic filter efficiencies	25
Table 4.5: Activated carbon and 400nm photocatalytic filter efficiencies for Bleach compounds	26
Table 4.6: Division of Experiment A10 into multiple periods and comparison to values from activated carbon and photocatalytic filter experiments	29
Table A1: Summary of experimental conditions and filter removal efficiencies from phase 1 experiments	43
Table A2: Summary of experimental conditions and filter removal efficiencies from phase 2 experiments ^{c,d,e}	44

List of Figures

Figure 2.1: Adsorption and photocatalysis hybrid system.....	9
Figure 3.1: Diagram of key flows in filter chamber experiments.....	19
Figure 3.2: Raw and log-normalized signal for methyl ethyl ketone from Experiment A2.....	21
Figure 4.1: Log-normalized signal and linear fits from Experiment 10	28
Figure 4.2: Time variant filter efficiencies for Experiment A10 based on 5-minute segmented linear regressions	30
Figure 4.3: Summary of time-variant filter removal efficiencies for Experiments A1- A9. Generated using 5-minute period linear regressions.....	31
Figure 4.4: Time-variant 5-minute segmented filter efficiencies for Experiment A7	32
Figure 6.1: Timeseries of NR-PM ₁ Species in from summer to fall 2020.....	38
Figure 6.1: Average seasonal compositions of NR-PM ₁ Species from 2020	39
Figure 6.3: Average seasonal compositions of total NR-PM ₁ from 2020	40
Figure 6.4: Fractional seasonal compositions of total NR-PM ₁ from 2020.....	40
Figure 6.5: Average diurnal profiles of total NR-PM ₁ from 2020.....	41

Chapter 1: Introduction

Indoor air quality refers to the quality of the air in an indoor environment. These environments include homes, schools, churches, and any other building environments. According to the U.S. Environmental protection agency's 1989 report, an average American spends about 90% of their time indoors (U.S. EPA, 1989). Typically, the concentrations of indoor air pollutants are twice to five times their concentrations in the outdoor environment (U.S. EPA, 1987; U.S. EPA, 1989). The combination of high pollutant concentrations and long lengths of time spent indoors leaves one vulnerable to exposure of indoor air pollutants and susceptible to the adverse health effects caused by such exposures.

Pollutant sources indoors include building materials, furniture, pets, office equipment, HVAC systems, humans as well as various human activities such as cooking and cleaning (Wargocki et al., 2004). These pollutants degrade air quality, cause health problems (Fang et al., 2002; Skov and Valbjorn, 1987; Sundel et al. 1991) and have been shown to reduce the performance of office work (Wargocki et al., 1999).

Numerous methods for reducing pollution in indoor environments have been explored. The pollution can be managed by confining the source or removing it from the environment, which necessitates that pollution sources can be identified and removed, 2) enhanced ventilation by increasing the amount of outdoor air entering the indoor environment resulting in the dilution of the pollutants indoors, which works against the aim for energy efficient buildings and 3) air purification or treatment technologies(Luengas et al., 2015).

Air purification or treatment technologies are believed to be the most achievable, cost efficient and energy efficient way of managing indoor air pollution. These

technologies can range from simple filters to more complex hybrid filters and are broadly classified into single and hybrid treatment techniques. Single treatment techniques include adsorption, mechanical filtration, photocatalytic oxidation (PCO), etc. and hybrid techniques include hybrid ozonation systems, adsorption and photocatalysis, etc. (Luengas et al., 2015).

For the purpose of this work, two single and one hybrid technique are explored: adsorption using an activated carbon filter, photocatalytic oxidation using a PCO filter and the adsorption and photocatalysis hybrid system using both filters in combination. The removal efficiencies are calculated using a simple indoor air quality model and compared. The influence of UV intensity, pollutant concentration, pollutant type, chamber size, air change rates and the efficiency in removing non-VOC pollutants are also explored.

The objectives of this work are:

1. To evaluate the filter removal efficiency of VOCs by an activated carbon filter.
2. To evaluate the filter removal efficiency of VOCs by a photocatalytic filter at two wavelengths of 345 nm and 400 nm
3. To evaluate the filter removal efficiency of an expanded set of VOCs by the photocatalytic filter at the more efficient wavelength (found to be 400 nm).
4. To evaluate the filter removal efficiency of VOCs a combined adsorption and photocatalytic oxidation filter operated at the more efficient wavelength.
5. To evaluate the filter removal efficiency of a mixture of bleach disinfectant and VOCs using the photocatalytic oxidation filter and a combined adsorption and photocatalytic oxidation filter at 400nm wavelength

In all experiments, filters were placed in a modified Bissell400 air purifier unit.

To achieve these objectives a total of 20 experiments split into two phases were run in environmental chambers with operating conditions mimicking that of a typical indoor environment. Subsequent chapters review literature on what has been explored in photocatalytic oxidation filters to date, the methods and experimental setup used in these experiments, a summary of results and conclusions and recommendations.

Chapter 2: Background

2.1 INDOOR AIR QUALITY

Indoor air quality is dependent on the composition and concentration of the contaminants in an indoor environment. Contaminants can be gases, particles or microorganisms. An indoor environment is described as having poor air quality when the contaminants in the space result in the discomfort of the occupants. For the context of this study the occupants of concern are humans and air quality can be described as poor when it is detrimental to human health. The importance of IAQ is continually emphasized because people spend between 80-95% of their lifetime indoors taking into account the amount of time spent in indoor environments such as schools, offices, hospitals, homes, etc. However, the majority of time spent indoors is spent in the home(Hedge, 2016).

Indoor pollutant concentrations are 2-100 times higher than outdoor concentrations with their sources being from outdoor and indoor sources. Indoor pollutants originate from human activities like cleaning, cooking, smoking etc., building materials, electronic equipment, furniture and comprise organic species and inorganic species in the gas and particle phase. Organic pollutants are typically a mix of at least 6000 compounds making it a difficult task to identify all pollutants of concern. Known hazardous pollutants can be managed via air cleaning or treatment techniques and by controlling the emissions from the sources. Control of emission sources have proven difficult and a less effective method of management as all the sources cannot be identified and isolated(Hedge, 2016).

According to the WHO (2000), pollutants known to have toxic effects on humans include carbon monoxide (CO), nitrogen dioxide (NO₂), sulfur dioxide (SO₂), PM₁₀ (particulate matter smaller than 10 micrometers in diameter), PM_{2.5}, ozone, benzene,

trichloroethylene, tetrachloroethylene, toluene, styrene, xylene, naphthalene, formaldehyde and polycyclic aromatic hydrocarbons (PAHs).

2.2 CLEANING INDOOR AIR

Strategies ranging from prevention to remediation have been applied to improve indoor air quality. Prevention strategies which involve the removal, confinement or replacement of the pollution source have proven to be insufficient in the attempt to purify indoor air. Another strategy aims at increasing the dilution of indoor air pollutants by increasing ventilation (Zaatari et al. 2014). This method can be effective in reducing the concentration of some pollutants but also carries the risk of exposing occupants to a different set of (outdoor) pollutants and poses a challenge to the energy efficiency of buildings (Chithra & Shiva Nagendra, 2012). Finally, a third strategy, which targets remediation, involves using purification or treatment technologies (Luengas et al., 2015). Air cleaning devices need to be used when the control or reduction of emissions from their sources cannot be achieved. Such devices may be as simple as filters or more complex hybrid treatment systems.

Mechanical filtration is one such simple filter used for air purification involving the removal of suspended particles by filters fitted into the heating, ventilation and air conditioning (HVAC) systems in buildings. Some filter types and their efficiencies at removing particles of 0.3-6 μm include flat filters with <5 %, pleated filters with a range of 20-50 % and a high efficiency particle arresting (HEPA) filter at >95% (Luengas et al., 2015). HEPA filters are currently the most used filters for the removal of particles indoors. Mechanical filtration has been used for the removal of ozone with efficiencies of about 36% (Zhao et al., 2007). However, the spent filter fittings present a new source of contamination as they may promote the growth of unsafe microorganisms(Luengas et al.,

2015). Electronic filtration is also a simple treatment system for the removal of particles in indoor air by the use of electrostatic precipitators or ionizers (Luengas et al., 2015).

Other simple treatment systems include adsorption, ozonation, UV photolysis, photocatalytic oxidation, cold plasma or non-thermal plasma (NTP), biofiltration, botanical purification and membrane separation. More complex combined systems are plasma-catalytic hybrid system, biological process and photocatalytic oxidation hybrid system, biological process and adsorption hybrid system, adsorption and photocatalysis hybrid system and hybrid ozonation systems.

2.2.1 Adsorption

Adsorption as an air cleaning technique physically removes pollutants from indoor air when they adhere to solid adsorbents(Chen et al., 2005). The technique has successfully retained air pollutants on the surface of the adsorbent material. Activated alumina, mineral clay, silica gel, activated carbon and zeolites are well known materials used for adsorption(Luengas et al., 2015). Porous activated carbon and hydrophobic zeolites are the most predominantly used adsorbents due to their high adsorption capacity and large surface area (Huang et al., 2003). Adsorption processes are hallmarked by a porous medium having high adsorptive capacity increasing the surface area(Das et al., 2004).

Activated carbon (AC) filters can be synthesized as granular activated carbon or activated carbon fibers (Bhave & Yeleswarapu, 2020). Granular activated carbon (GAC) type filters are produced by crushing carbon particles resulting in granules between 0.2-5 mm and granules in the 15–25micron size range may be referred to as powdered activated carbon (Aktas & Cencen, 2012). Of the two size ranges of granular activated carbon, the 0.2-5 mm size range is preferred because of its larger surface area. Wood, coal and coconut

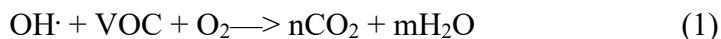
shells are the major precursors for the production of GAC and other agricultural waste products may also be used for this purpose (Bansal et al., 2005; Haghghat et al., 2008).

Activated carbon fibers (ACF) are considered to be more promising than granular activated carbon due to their high surface area and macro-pore size distribution. A combination of these factors makes the adsorption capabilities higher (Das et al., 2004). ACF can also be electrothermally regenerated giving it a higher advantage over GAC. Synthesis of ACF is usually achieved from textile fabrics and numerous other precursors and the pore structure is influenced by the nature of the fabric weave (Sidheswaran et al., 2012)

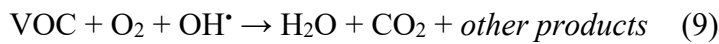
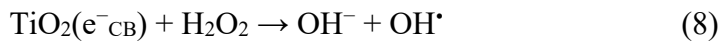
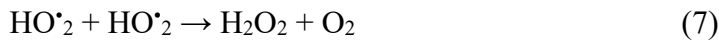
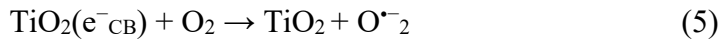
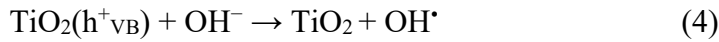
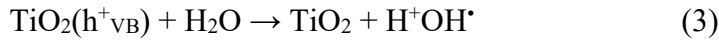
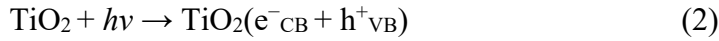
Efficiency of AC filters is affected by the surface structure of the activated carbon, surface chemistry which depends on the precursor, activating procedure and agents, temperature which has been seen to decrease the efficiency of the removal of toluene when increased, relative humidity and the presence of ozone. Relative humidity affects both the removal efficiency of VOCs and the life of activated carbon. Higher relative humidity reduces the performance and may cause the growth of microbes on the surface of the AC (Jo & Yang, 2009).

2.2.2 Photocatalytic Oxidation

Photocatalytic oxidation is a chemical process which involves the use of ultraviolet radiation to activate a catalyst which converts VOCs to CO₂ and water. There are several options of catalysts to be used for PCO; however, the most widely used catalysts are nano-titania or titanium dioxide (TiO₂), which has been widely used in most of the published work on photocatalytic oxidation and zinc oxide (ZnO) (Mo et al., 2009). The net PCO reaction is written as:



A more comprehensive mechanism of PCO using TiO₂ is shown below (Haghighat et al., 2016):



Air purification via PCO is attractive because it is safe, a mild oxidant, active at room temp, and the hydroxyl radical is a universal oxidant able to oxidize a broad range of compounds. As all catalysts, photocatalysts can be deactivated. The lifetime of a photocatalyst greatly influences the economics of this method of treatment. Deactivation primarily results from the loss of active sites which are the effect of formation of byproducts or intermediates, photopolymerization of some species (e.g., benzene) on the surface, complete photocatalytic oxidation of some species and accumulation of these oxidized forms on the surface (Mo et al., 2009).

2.2.3 Adsorption and photocatalysis

Photocatalysis can be used in combination with adsorption as a hybrid treatment technique. Adsorption is added as a step in the process where pollutants are adsorbed on the surface of the adsorbent and then they are oxidized by a photocatalyst as shown in figure 2.1. Combined methods have been observed to improve the removal efficiencies of filters. Jo & Yang (2009) tested a combined filter system and compared it to the removal

efficiency of an adsorption only system. The combined system was made up of an activated carbon adsorption layer and a photocatalytic oxidation layer. They used the hybrid treatment system on a mixture of benzene, toluene, ethylbenzene and xylene (BTEX) at typical indoor concentration levels.

Activated carbon and photocatalytic oxidation (AC-PCO) hybrid system had removal efficiencies near 100% higher than the removal efficiencies of the AC filter alone which was about 90% (Jo & Yang, 2009). The results obtained in this experiment are comparable to results obtained from Ao & Lee (2004) in their studies of immobilized photocatalyst on AC filters. Results from this study show an increased removal efficiency in AC-PCO filters and a reduction in the production of NO_2 as a byproduct.

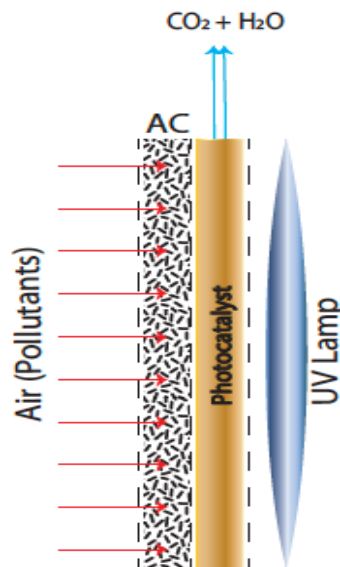


Figure 2.1: Adsorption and photocatalysis hybrid system

2.3 PHOTOCATALYTIC OXIDATION AIR PURIFIERS

In evaluating the performance of ultraviolet photocatalytic oxidation (UVPCO) for indoor air cleaning applications, Hodgson et al. (2007), found that the device with 33%

conversion efficiency for VOCs produced indoors would remove as much VOC as ventilation. However, this effect is counteracted by increased airflow rate resulting in ventilation overtaking the efficiency of the device. Low removal efficiencies of chlorinated species were noted but not reviewed further because the species were said to be less prominent in indoor spaces, however with the COVID19 pandemic the use of chlorinated disinfection products has been on the rise and a corresponding increase in the presence of chlorinated species in indoor environments has been observed. Production of formaldehyde, acetaldehyde, formic acid and acetic acid was recorded during their experiments. The UVPCO device in their study was installed in a HVAC system (Hodgson et al., 2007).

The photocatalytic degradation of VOCs using a short wavelength light of 254nm and ozone was investigated by Sekiguchi et al. and a high removal efficiency of toluene was observed both while irradiated and not. Removal of toluene was higher at 185nm wavelength and in wet conditions. However fine particles were formed that could have adverse health impacts (Sekiguchi et al., 1999).

Kim et al. (2009), studied the photocatalytic degradation of VOCs at the interface of a titanium dioxide catalyst. They studied the degradation of toluene among others in a batch reactor and perturbed the conditions by adjusting water vapor, molecular oxygen and reaction temperature. Water vapor improved toluene degradation and hindered the degradation of the other VOCs like acetone. Oxygen was determined to be an essential component in photocatalytic oxidation because it holds the generated electrons on the surface. Minor changes in temperature had no effect on the system, but a compound dependent change was observed when temperatures between the range 25 - 75°C were investigated. Acetone, toluene and methanol all had the lowest reaction rates at the highest temperature of 75°C (Kim, 2009).

In this study, nearly undetectable removal efficiencies were recorded for chlorinated species which are byproducts from the cleaning of indoor spaces with a typical bleach disinfectant mixture.

2.3.1 Parameters influencing photocatalytic oxidation

Airflow rate and residence time, concentration of pollutant, relative humidity and light source and intensity are the major factors influencing the efficiency of the photocatalytic oxidation process. Residence time of pollutants in the reactor plays a major role in the removal efficiency of PCO air filters. An increase in residence time showed a simultaneous increase in the removal efficiency of BTEX (Ao & Lee, 2004). Typically, an optimal concentration exists for the pollutant at which the photocatalytic oxidation rate is maximized, and mixtures of VOCs were found to have no effect on filter efficiency (Mo et al, 2009). An optimal relative humidity exists for maximal operation of the photocatalyst (Mo et al, 2009). Increased humidity decreased the removal efficiency of BTEX in studies from Ao & Lee (2004).

Temperature affects both the reaction rate of the photocatalyst as well as compound adsorption of the surface of the photocatalyst. Kinetic reaction rate constant follows an Arrhenius equation highlighting its temperature dependence and adsorption equilibrium constant is affected as an increase in temperature reduces the amount of a compound adsorbed on the surface of the photocatalyst. PCO reaction rate is a function of both the adsorption and the kinetic reaction rate, increasing temperature will increase the reaction rate to a maximum and then drop. This occurrence suggests an optimal temperature exists for operating the photocatalyst and this is at the point where the maximum reaction rate is observed (Mo et al, 2009).

Theoretically, ultraviolet wavelengths less than 380nm should be sufficient for activating titania photocatalysts (Mo et al, 2009).

2.3.2 Existing Filters

In a study by ASHRAE in the performance of air cleaners for removing multiple VOCs, portable air cleaners and HVAC fitted air cleaners were used. Adsorption filters were found to be the most efficient at removal of VOCs and UVPCO type filters, if well designed, were seen as a promising method of air cleaning. However, the use of ionizers or ozone generating type air filters was discouraged as byproducts generated with these techniques pose high human health risks (Chen et al., 2005).

2.4 SCOPE OF THIS WORK

This work investigates the compound specific removal efficiency of a novel photocatalyst air filter at removing single volatile organic compounds (VOCs), a mixture of VOCs and a mixture of VOCs and disinfection products in a typical indoor environment. It goes further to compare the removal efficiency of the photocatalyst filter, an activated carbon filter and a combination of the photocatalyst and activated carbon filters.

Experiments were conducted in environmental chambers at the J.J. Pickle Research Campus at the University of Texas at Austin. Operating conditions in the chambers were representative of indoor environments. Known concentrations of methyl ethyl ketone, toluene, α -pinene, D5-siloxane and octyl aldehyde and a mixture of methyl ethyl ketone, α -pinene and butyric acid were injected into the chamber and allowed to mix for 10 minutes. The compounds were then allowed to decay for 10 minutes to determine the background loss rate (“filter off” loss rate). The Bissell400 air purifier unit fitted with either the photocatalytic oxidation filter or activated carbon filter, or both was then turned

on and allowed to run for 30 minutes to establish the filter on loss rate. The “filter on” and “filter off” loss rates were then compared to determine the compound specific filter efficiency using procedures discussed further in the methods section.

Chapter 3: Materials and Methods

3.1 DECAY TESTING

Tests were performed in a 14 m³ and 67 m³ stainless steel chamber for phase 1 and phase 2 respectively. The chambers are located at UT Austin's JJ Pickle Research Campus. For the phase 2 experiments, the chamber was set up to simulate a typical classroom with 6 tables, 2 painted wallboards and a thermal manikin. An average expected air exchange rate of 1 was targeted and the air exchange rate was calculated for each experiment based on the decay of non-reactive, non-adsorbing tracer species including CO₂ and difluoroethane. Based on CO₂ data, the average air exchange rate of the chamber in phase 1 experiments was $0.86 \text{ h}^{-1} \pm 0.05 \text{ h}^{-1}$ and for phase 2 experiments was $0.97 \text{ h}^{-1} \pm 0.12 \text{ h}^{-1}$ (average values here are presented \pm standard deviation). The chamber was also well mixed by the addition of a plastic stand fan in phase 1 and with the aid of the fan in the modified Bissell400 air purifier unit in phase 2. Injection and gas sampling from the chamber utilized teflon tubing run into the chamber.

The filter unit utilized in this testing was a modified Bissell air400 purifier unit. It included a high-efficiency particulate absorbing (HEPA) filter and was usually equipped with an activated carbon filter. The unit was modified with additional power electronics for LED lights and use of the photocatalytic filter trays. An unmodified unit was used for activated carbon testing in phase 1 while phase 2 utilized the modified unit for all experiments. Major variables associated with the filter unit included flow rate setting which could range from 25 to 107 liters per minute (LPM) and the wavelength produced by the LEDs which could be either 365 or 400 nm light.

Decay tests involve injecting a compound into the chamber with the filter unit off. After allowing the compound concentration to decay to obtain a background loss rate, the

filter unit was turned on. By comparing the loss rate in the “filter off” period to the “filter on” period, compound specific filter efficiencies can be calculated according to the procedure described under data analysis. Other information from these tests includes dependency of filter removal efficiency on wavelength, flow rate, and pollutant concentration, and information regarding compounds off-gassing from the filter prior to injection. A summary of testing conditions and experiments for phase 1 and 2 is shown in Table 1 and 2 respectively. Experiments tagged “A” refer to phase 1 and “B” refer to phase 2.

3.2 INSTRUMENTATION

Data presented here was collected using a Vocus high resolution, time of flight, proton transfer reaction mass spectrometer (Vocus 2R-PTRToF-MS or Vocus, Aerodyne Inc.), a Time-of-Flight Chemical Ionization Mass Spectrometer operating in Iodide mode (I-CIMS, Aerodyne Inc) and the LI-COR for detecting CO₂. The Vocus has a limit of detection < 1 ppt, with a mass resolving power < 1 mDa (Wang et al., 2020). It utilizes H⁺ ions to form adducts with gas phase compounds and separates these charged adducts by mass to charge (m/z) ratio through electrodynamic lenses and a long time of flight region. This high-resolution instrument can identify multiple compound peaks at a single m/z. Therefore, specific injected compounds can be well identified, and their decay can be tracked without interference from other compounds. In addition, compounds which are off-gassed from the filter or are present in the background can be identified.

Iodide-adduct time of flight chemical ionization mass spectrometer (I-CIMS) was used to detect and track the decay of chlorinated species from the bleach cleaning conducted simultaneously with VOC injections. This instrument is well suited for measuring a wide array of highly oxidized and chlorinated species with minimal

fragmentation and allows measurement of highly functionalized low volatility and reactive compounds. It also has high sensitivity, selectivity and time resolution (Wang et al., 2020). CO₂ and H₂O concentrations were measured using a LI-COR LI-850 CO₂/H₂O gas analyzer. CO₂ concentration was used to determine air exchange rate. H₂O levels were not controlled but averaged 47% ± 20% RH for the duration of both experiments.

Table 3.1: List of experimental conditions for phase 1 decay testing

Exp #	Filter type	Layers	Wavelength (nm)	Filter flow rate (LPM)	Compounds tested
A1	Activated Carbon	2	--	107	Toluene
A2	Activated Carbon	2	--	25	Methyl ethyl ketone Octyl aldehyde α -pinene
A3	Activated Carbon	1	--	25	D5-siloxane
A4	Photocatalytic	2	365	107	Toluene
A5	Photocatalytic	2	365	25	Isopropyl alcohol
A6	Photocatalytic	2	365	25	Octyl aldehyde α -pinene
A7	Photocatalytic	2	400	25	Methyl ethyl ketone Octyl aldehyde α -pinene
A8	Photocatalytic	2	365	107	Methyl ethyl ketone Octyl aldehyde α -pinene
A9	Photocatalytic	1	365	25	D5-siloxane
A10	Photocatalytic & activated carbon	2	365	25	Methyl ethyl ketone Octyl aldehyde α -pinene

Volatile organic compounds utilized in these experiments included toluene, octyl aldehyde, methyl ethyl ketone (MEK or 2-butanone), α -pinene, isopropyl alcohol, decamethylcyclopentasiloxane (D5), butyric acid and Clorox bleach disinfectant. The VOCs were sourced from Sigma Aldrich at high purity and Clorox bleach was purchased at a local store. Some D5-siloxane testing was conducted using D5-siloxane from a spray-on deodorant (Degree Men in scent “Cool Rush”). CO₂ was from a 99% purity Praxair cylinder and difluoroethane was from an air duster can.

Table 3.2: List of experimental conditions for phase 2 decay testing

Exp #	Filter type	Layers	Compounds tested
B1	Photocatalytic	1	Bleach
B2	Activated Carbon	2	Bleach
B3	Photocatalytic & Activated Carbon	2	Bleach
B4	Photocatalytic	1	VOC mixture
B5	Photocatalytic & Activated Carbon	2	VOC mixture
B6	Photocatalytic	1	Bleach + VOC mixture
B7	Activated Carbon	2	Bleach + VOC mixture
B8	Photocatalytic & Activated Carbon	2	Bleach + VOC mixture
B9	Photocatalytic & Activated Carbon	2	Bleach + VOC mixture
B10	Photocatalytic & Activated Carbon	2	Bleach + VOC mixture

VOC mixture = Methyl ethyl ketone + α -pinene + Butyric acid

3.3 EXPERIMENTAL SET UP

Tests conducted in phase 1 of the experiments involved the injection of a single VOC species into a 14 m³ environmental chamber. The VOCs used here were toluene,

octyl aldehyde, methyl ethyl ketone (MEK or 2-butanone), α -pinene, isopropyl alcohol and decamethylcyclopentasiloxane (D5). CO₂ was injected into the chamber to enable tracking and calculation of the air change rate during the experiments. The order of experiments and specific VOC species injected into the chamber is indicated in table 3.1

Phase 2 experiments involved the injection of a calculated mass of a VOC mixture into a 67 m³ stainless steel chamber with the targeted total concentration of 200ppb. A mix of methyl ethyl ketone, α -pinene and butyric acid were injected into the chamber during the VOC only runs. During the combined bleach and VOC runs, concentrated bleach was diluted with water in a humidifier and turned on for the duration of the experiment which ran for 30 – 60 minutes. CO₂ was also injected into the chamber to enable tracking and calculation of the air change rate during the experiments. These experiments were modified to test only UV lights at 400 nm after results from phase 1 showed the photocatalyst when irradiated with 400 nm UV lights had a higher removal efficiency.

3.4 DATA ANALYSIS

A simple indoor air mass balance as shown in figure 3.1 was used in calculating the concentrations of the compounds injected into the chamber in these experiments.

In Figure 3.1 and equations 1 to 4b, C_{out} is the concentration of the compound of interest outside the chamber (generally 0, but 400 ppm for CO₂). C is the concentration of the compound of interest inside the chamber. Q is the bulk flow rate through the chamber. V is the volume of the chamber. k is the loss rate of the compound of interest to surfaces. η is the efficiency of the filter and Q_f is the volumetric flow rate through the filter with the values shown in table 3.3. The appropriate mass balance for a particular compound in this system is shown in equation 3.1.

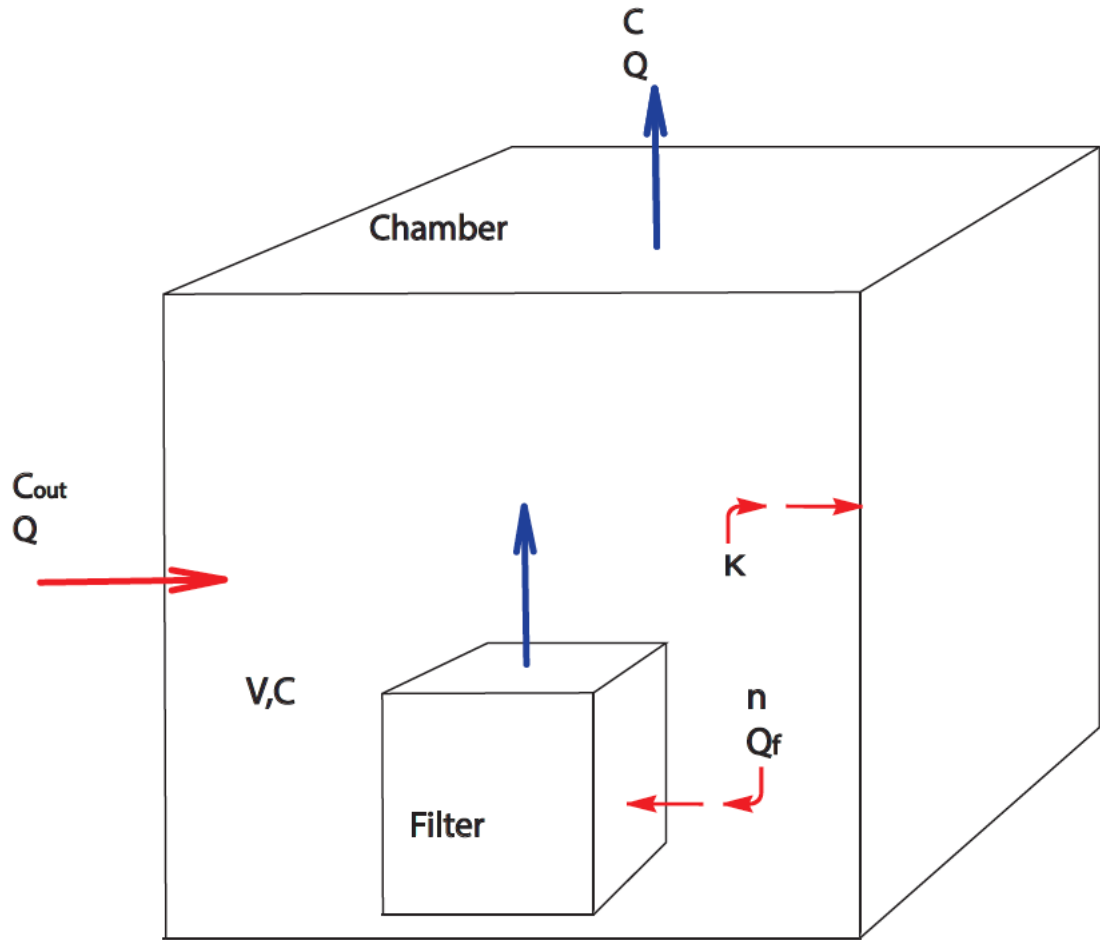


Figure 3.1: Diagram of key flows in filter chamber experiments

$$V \frac{dC}{dt} = QC_{out} - C(Q + kV + \eta Q_f) \quad \text{Equation 3.1}$$

Dividing by V and defining $\frac{Q}{V}$ as λ (this is the air exchange rate), we arrive at equation 3.2.

$$\frac{dC}{dt} = \lambda C_{out} - C(\lambda + k + \eta \frac{Q_f}{V}) \quad \text{Equation 3.2}$$

Then, evaluating from $t = 0$ to $t = t$ and defining $C = C(t)$ and $C_0 = C(t=0)$ and extracting constants results in Equation 3.3.

$$-\ln\left(\frac{C_{\text{out}}-C}{C_{\text{out}}-C_0}\right) = \left(\lambda + k + \eta \frac{Q_f}{V}\right)t + C \quad \text{Equation 3.3}$$

Equation 3.3 indicates that a linear regression of $-\ln\left(\frac{C_{\text{out}}-C}{C_{\text{out}}-C_0}\right)$ against t will result in a line with a slope of $\lambda + k + \eta \frac{Q_f}{V}$. Given that C_{out} is known, C_0 is measured, C is measured, Q_f is known, and V is known this can easily allow extraction of λ , k and η .

Table 3.3: Volumetric flowrate, Q_f , through the filter

Fan Setting	Q_f (Liters per minute)
Silent	25
Low	38
Medium	58
High	74
Max	107

For CO_2 data, we assume that $k=0$ and $\eta = 0$. We will assume $C_{\text{out}} = 400$ ppm, this can also be extracted from the pre- CO_2 injection data. Background air exchange rate can be extracted from the CO_2 decay curve.

For a specific VOC compound, we will assume that $C_{\text{out}} = 0$, and C_0 is extracted from the initial Vocus signal for that compound at a defined $t=0$. During a filter off period, we assume $\eta = 0$. The filter off equation (Equation 3.4a) will be used to calculate the background loss rate and the filter on equation (Equation 3.4b) will be used to calculate the filter loss rate and background loss rate.

$$-\ln\left(\frac{C}{C_0}\right) = (\lambda + k)t + C \quad \text{Equation 3.4a}$$

$$-\ln\left(\frac{C}{C_0}\right) = \left(\lambda + k + \eta \frac{Q_f}{V}\right)t + C \quad \text{Equation 3.4b}$$

By subtracting the filter-on slope from the filter-off slope $\eta \frac{Q_f}{V}$ can be extracted and filter efficiency is calculated. Surface loss rate (k) can be calculated by subtracting the air exchange rate from tracer decay from Equation 4a. An example of the raw and log-normalized signal from an experiment is shown in figure 3.2.

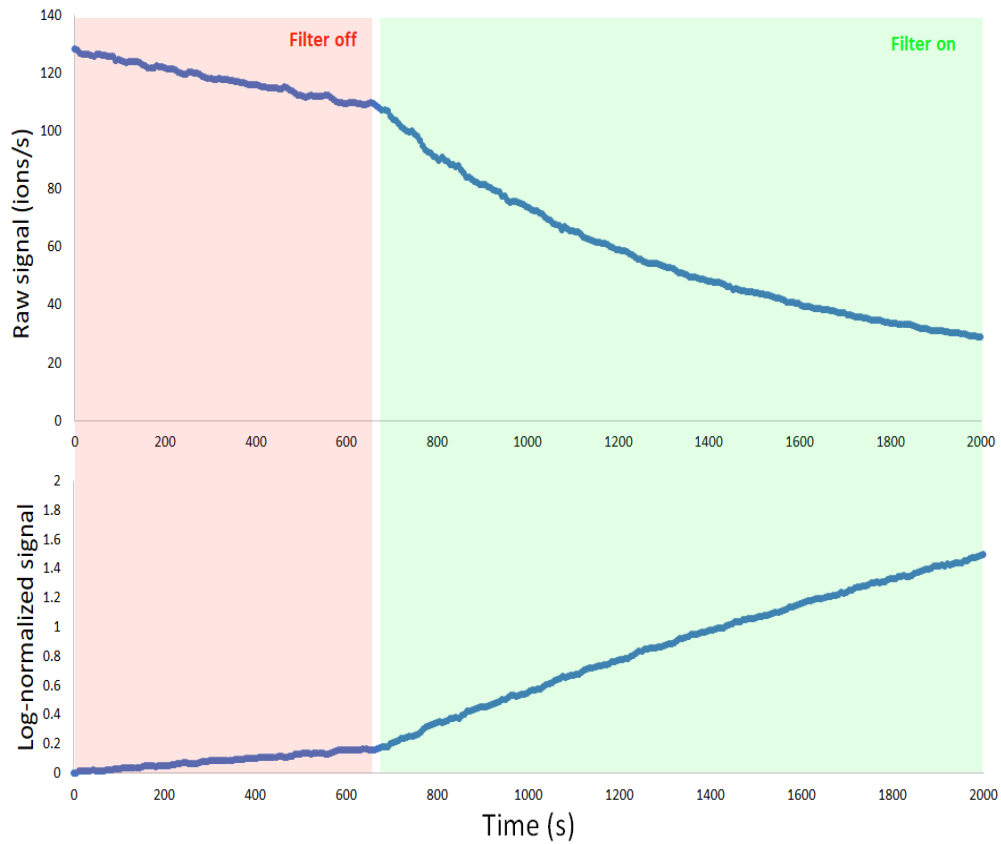


Figure 3.2: Raw and log-normalized signal for methyl ethyl ketone from Experiment A2

Chapter 4: Results and Discussion

4.1 PHOTOCATALYTIC OXIDATION AND ACTIVATED CARBON EFFICIENCIES

In all tested cases and all compounds from phase 1 experiments, activated carbon filter efficiency was higher than photocatalytic filter efficiency. In some cases, photocatalytic filter efficiency appears to be negligible (<1%) and will be reported as 0% efficiency. A clear comparison between activated carbon and photocatalytic filter efficiencies using 365 nm lights can be made for toluene (experiments A1 and A4), octyl aldehyde and α -pinene (experiments A2 and A6), and D5-siloxane (using experiments A3 and A9). A comparison between activated carbon and photocatalytic filter efficiencies using 400 nm lights for MEK, octyl aldehyde, and α -pinene can be made (experiments A2 and A7). Pairs of experiments listed here for comparison have the same filter flow rate setting on silent. These comparisons are summarized in Table 4.1.

Table 4.1: Comparison of activated carbon and photocatalytic filter efficiencies from phase 1 experiments

Compound	Filter type		
	Activated Carbon ^a	365 nm photocatalytic ^b	400 nm photocatalytic ^c
Toluene	15%	0%	
Methyl ethyl ketone	30%		2.70%
α -pinene	47%	0%	14%
Octyl aldehyde	45%	0%	6.30%
D5-siloxane	32%	7.6%	

^aActivated carbon measurements for toluene are from experiment A1, MEK, α -pinene, and octyl aldehyde from experiment A2, and D5-siloxane from experiment A3. ^b365 nm photocatalytic oxidation measurements for toluene are from experiment A4, α -pinene and octyl aldehyde from experiment A6, and D5-siloxane from experiment A9. ^c400 nm photocatalytic oxidation measurements for MEK, α -pinene, and octyl aldehyde from experiment A7.

It is clear from Table 4.1 that the activated carbon had a higher filter removal efficiency. In addition, at 365 nm the photocatalytic filter shows no significant efficiency

in removing toluene, α -pinene and octyl aldehyde. However, the 365 nm photocatalytic filter did remove D5-siloxane at 7.6% efficiency. The 400 nm wavelength photocatalytic filter removed methyl ethyl ketone, alpha pinene, and octyl aldehyde at a higher efficiency than the 365 nm photocatalytic filter, but still had a lower efficiency than the activated carbon filter. Theoretically UV wavelengths less than 380 nm have been said to be more suitable for activating photocatalysts (Mo et al., 2009), however, the 400 nm photocatalytic filter removed the VOCs at a higher efficiency than the 365 nm filter.

Activated carbon filters having the higher filter efficiency in comparison to the photocatalytic oxidation air purifier in these experiments is consistent with previous works showing that activated carbon typically has a higher removal efficiency than PCO air purifiers. However, there are differences between the AC filter in these experiments which have filter efficiencies 15 – 47% and those from Gallego et al. (2013) which recorded removal efficiencies of 70% for toluene and 74% for methyl ethyl ketone (Gallego et al., 2013).

4.2 COMPOUND SPECIFIC REMOVAL EFFICIENCIES FOR THE PHOTOCATALYTIC FILTER

The efficiency of the photocatalytic filter in removing specific VOCs and some compounds of interest from bleach disinfection (chlorine and hypochlorous acid) was tested and the results are summarized in Table 4.2. Results in Table 4.2 show that efficiency for all VOCs were within the range 5 - 40%. The removal efficiency of butyric acid was significantly higher than that of methyl ethyl ketone and α -pinene. Butyric acid had the lowest composition in the VOC mixture, pointing towards the possible efficiency in removing lower concentrations of VOCs in the chamber. However, removal of bleach disinfectant species was fairly low similar to Hodgson et al., (2007). In addition to removal

through air exchange and filtration, decreases in the concentrations of these species may also have been due to loss to surfaces, particularly as the surfaces may have been wet.

Table 4.2: Filter efficiencies of 400nm photocatalytic filter

Compound	Removal Efficiency	Experiment
Methyl ethyl ketone	8%	B4
α -pinene	12%	B4
Butyric acid	37%	B4
Cl ₂	< 5% ^a	B1
HOCl	LOD ^b	B1

^a< 5% indicates that the removal efficiency value calculated was low. Values <5% are highly uncertain and cannot be quantified reliably

^bLOD indicates that low measurement sensitivity and low concentrations make calculation of efficiency impossible

4.3 COMPOUND SPECIFIC REMOVAL EFFICIENCIES FOR THE ACTIVATED CARBON – PHOTOCATALYTIC OXIDATION HYBRID FILTER

Here the combined effect of the photocatalytic filter and activated carbon filter was studied. In some cases, the efficiencies were outside the range of detection (indicating a dominance of ventilation and losses to surfaces). VOC removal efficiencies are summarized in table 4.3 below. In experiment B5 (VOC only mixture), as seen in table 4.3, the removal efficiency of methyl ethyl ketone is similar to the efficiency in table 4.2 when the photocatalytic filter alone was in operation. The efficiency was higher in experiments 8 and 10.

Butyric acid exhibits a significantly higher removal efficiency when the photocatalytic and activated carbon filters are used. The last experiment, B10, had the lowest VOC mixture concentration and the highest removal efficiency. This is consistent with the higher removal efficiency of butyric acid which had the lowest concentration in the VOC mixture.

Table 4.3: Activated carbon and 400nm photocatalytic filter efficiencies for VOC mixture

Experiment	Compound		
	Methyl ethyl ketone	α -pinene	Butyric acid
B5	12%	<5% ^a	LOD ^b
B8	22%	<5% ^a	<5% ^a
B9	7%	17%	42%
B10	54%	73%	62%

^a< 5% indicates that the removal efficiency value calculated was extremely low. Values <5% are highly uncertain and are not distinguished from other low values in this paper.

^bLOD indicates that low measurement sensitivity and low concentrations make calculation of efficiency impossible

Overall, we see that the removal efficiencies observed in the combined filter is higher than the removal efficiencies observed for the photocatalytic filter for most of the VOCs. This outcome is not surprising taking phase 1 experiments into account where the activated carbon filter efficiencies were higher than the efficiencies from both the 365nm and 400nm photocatalytic filters (activated carbon efficiencies from phase 1 shown in table 4.4).

Table 4.4: Comparison of Phase one and Phase two 400 nm photocatalytic filter efficiencies

Compound	Phase 1		Phase 2	
	Photocatalytic oxidation ^c	Activated carbon	Photocatalytic oxidation	Photocatalytic oxidation and Activated carbon
Methyl ethyl ketone	2.70%	30%	8%	22% ^a
α -pinene	14%	40%	12%	17% ^b
Octyl aldehyde	6.30%	--	--	--
Butyric acid	--	--	37%	--

^aData from experiment B8

^bData from experiment B9

^cUV light wavelength 400 nm

For the experiments in which a mixture of bleach and VOCs were injected (B8, B9 & B10), and the experiment in which bleach only was injected (experiment B2), the removal efficiency of bleach associated compounds was investigated. The results from these experiments are summarized in table 4.5. In experiment B2, the activated carbon filter was run and returned efficiencies <5%. In experiments B8 - B10 the combined filter setup was used, and chloramine had efficiencies greater than 10% in two experiments. The improved removal of chloramine compared to chlorine and hypochlorous acid (both of which report <5% efficiencies) is worth noting. This may be related to the specific structure of the chloramine molecule, though further exploration using synthesized chloramine species would be required.

Table 4.5: Activated carbon and 400nm photocatalytic filter efficiencies for Bleach compounds

Experiment	Compound		
	Chlorine	Hypochlorous acid	Chloramine
2	< 5 % ^a	< 5 % ^a	<5% ^a
4	LOD ^b	LOD ^b	32%
9	< 5 % ^a	LOD ^b	LOD ^b
10	LOD ^b	LOD ^b	17%

^a< 5% indicates that the removal efficiency value calculated was low. Values <5% are highly uncertain and cannot be quantified reliably

^bLOD indicates that low measurement sensitivity and low concentrations make calculation of efficiency impossible

4.4 UNCERTAINTIES RELATED TO EXPERIMENTAL SET UP AND LOW EFFICIENCY FILTRATION

There are limitations to these experiments and this experimental design due to high uncertainties associated with low flows and low removal efficiencies. For a filter operating at the low flow rate setting of the Bissell air400 unit (38 LPS or 136.8 m³ h⁻¹), the clean air

delivery rate (CADR) associated with a moderate removal efficiency (assume 50%) is $68.4 \text{ m}^3 \text{ h}^{-1}$. At this point, that CADR is nearly identical to the ventilation rate through the chamber in this study. A small change in the ventilation rate or the filter flow rate would significantly impact the calculated removal efficiency, even for 50% efficient filters. The largely lower efficiencies described here provide even greater uncertainty as they are dwarfed by the impact of ventilation. Furthermore, reducing the ventilation rate, air exchange rate, or size of the chamber, while potentially helpful, will not reduce uncertainty sufficiently for extremely low efficiencies. Data from three experiments (A3, A6 and A7) could not be used to calculate filtration efficiencies due to issues with the sampling set-up on those days.

4.5 COMBINED FILTER NON-LINEARITY

Experiment A10 was a combined filter experiment with one layer of photocatalytic filter media energized by 365 nm wavelength light and one layer of activated carbon media. The filter was arranged such that incoming air first contacted the photocatalytic filter. Methyl ethyl ketone, octyl aldehyde and α -pinene were injected during this decay experiment. Filter removal efficiencies in this test for methyl ethyl ketone, octyl aldehyde, and α -pinene were 5.5%, 0%, and 11% respectively. However, this experiment highlights how filter removal efficiency can be time-variant. In this experiment and others, the log-normalized signal is not linear (Figure 4.1). The linear relationship defined in the mass balance for filter efficiency does not adequately describe the full filter on period. While applying a linear regression to the full period provides a reasonable average filter efficiency, segmenting the data into different time periods reveals how filter efficiency changes over time. The results of this treatment and comparison to other experiments are

shown in Table 4.6 while a time-variant presentation of 5-minute segmented filter efficiencies is shown in Figure 4.2.

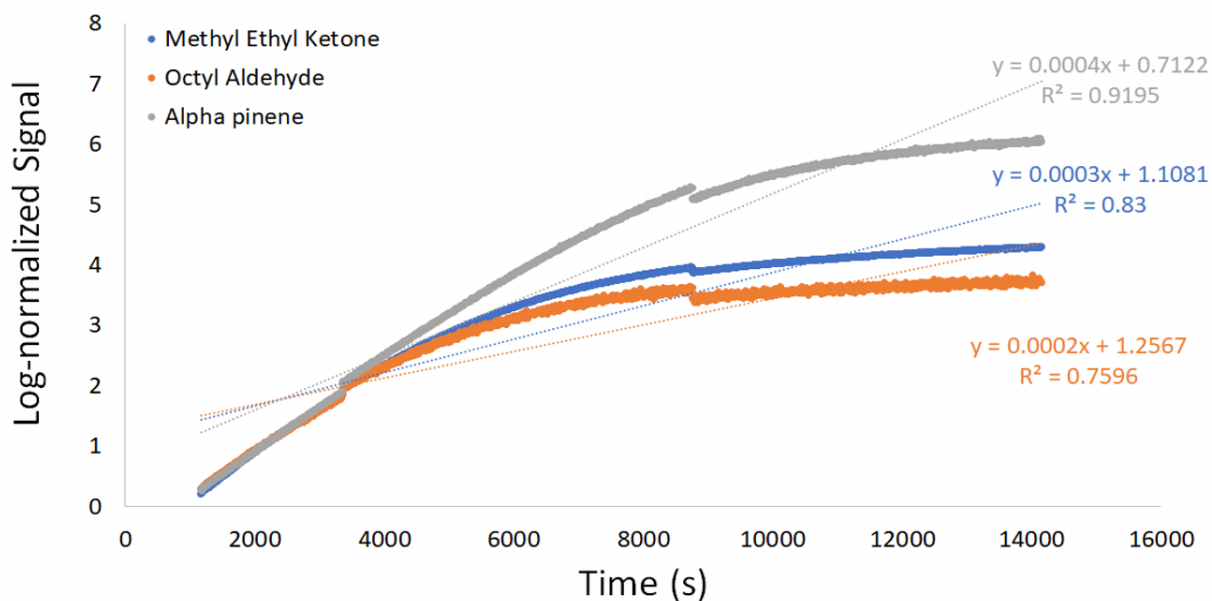


Figure 4.1: Log-normalized signal and linear fits from Experiment 10

Table 4.6 and Figure 4.2 indicate that the initial period has a high removal efficiency, similar to activated carbon alone, but later periods decrease in efficiency. The negative efficiencies in the third period here seem to indicate some emission of these compounds compared to background loss rate. However, these negative values may fall within the uncertainty of efficiency measurements at low concentrations. It is possible that this nonlinear behavior is indicative of filter capacity being reached or some form of filter poisoning. Future tests with intentionally poisoned or saturated filters could illuminate some drivers of filter efficiency shifts.

Table 4.6: Division of Experiment A10 into multiple periods and comparison to values from activated carbon and photocatalytic filter experiments

Compound	Experiment A10				Experiment A2 ^a	Experiment A7 ^b
	Full Experiment	First Period	Second Period	Third Period	Activated Carbon	400 nm photocatalytic
Methyl Ethyl Ketone	5.5%	32%	10%	-6%	30%	2.7%
α -pinene	11%	28%	21%	-5%	47%	14%
Octyl aldehyde	0%	25%	2.6%	-11%	45%	6.3%

^aExperiment A2 utilizes 2 layers of activated carbon.

^bExperiment A7 uses 400 nm photocatalytic oxidation but is presented to indicate the maximum photocatalytic filter removal for these compounds.

This nonlinear behavior occurs in some other experiments during the filter on period, and time variant filter efficiencies for other experiments are included in Figure 4.3. However, the 400 nm wavelength excited photocatalyst in Experiment A7 has a unique behavior. As shown in Figure 4.4 below, filter removal efficiencies for this experiment increase over time, indicating an inverse relationship between filter efficiency and concentration. This relationship requires more detailed probing, but it is possible that this filter removes compounds at a constant mass rate as opposed to a constant proportion and this drives a variable efficiency relationship. In general, this variable filter efficiency calls into question the appropriate metric for evaluating these filters. While overall filter efficiency is chosen here based on general literature, alternate measures such as initial filter efficiency, maximum filter efficiency, or mass filtration rate should be explored in the future.

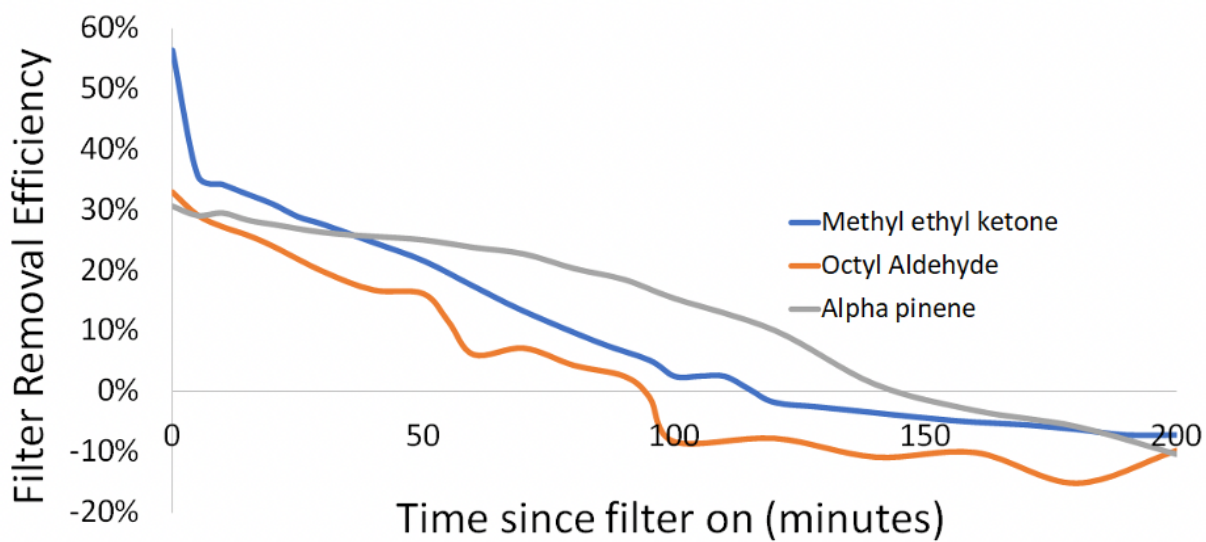


Figure 4.2: Time variant filter efficiencies for Experiment A10 based on 5-minute segmented linear regressions

4.6 FILTER EFFICIENCY DEPENDENCE ON FLOW RATE, COMPOUND CONCENTRATION AND WAVELENGTH

As mentioned above, photocatalytic oxidation using 400 nm wavelength light resulted in higher removal efficiency than photocatalytic oxidation using 365 nm wavelength light. In planning and conducting these experiments, theory suggests that lower UV wavelengths are more suitable for photocatalysts (Hodgson et al., 2009) hence the 365 nm light was expected to result in better removal efficiency than 400 nm lights due to the higher energy of 365 nm lights. Given this understanding, only one reasonably comparable 400 nm wavelength experiment was conducted. In literature, longer wavelengths tend to reduce photocatalytic oxidation rates and effectiveness (Xingzhou, 1997; Zhang, 1996; Driessen & Grassian, 1998).

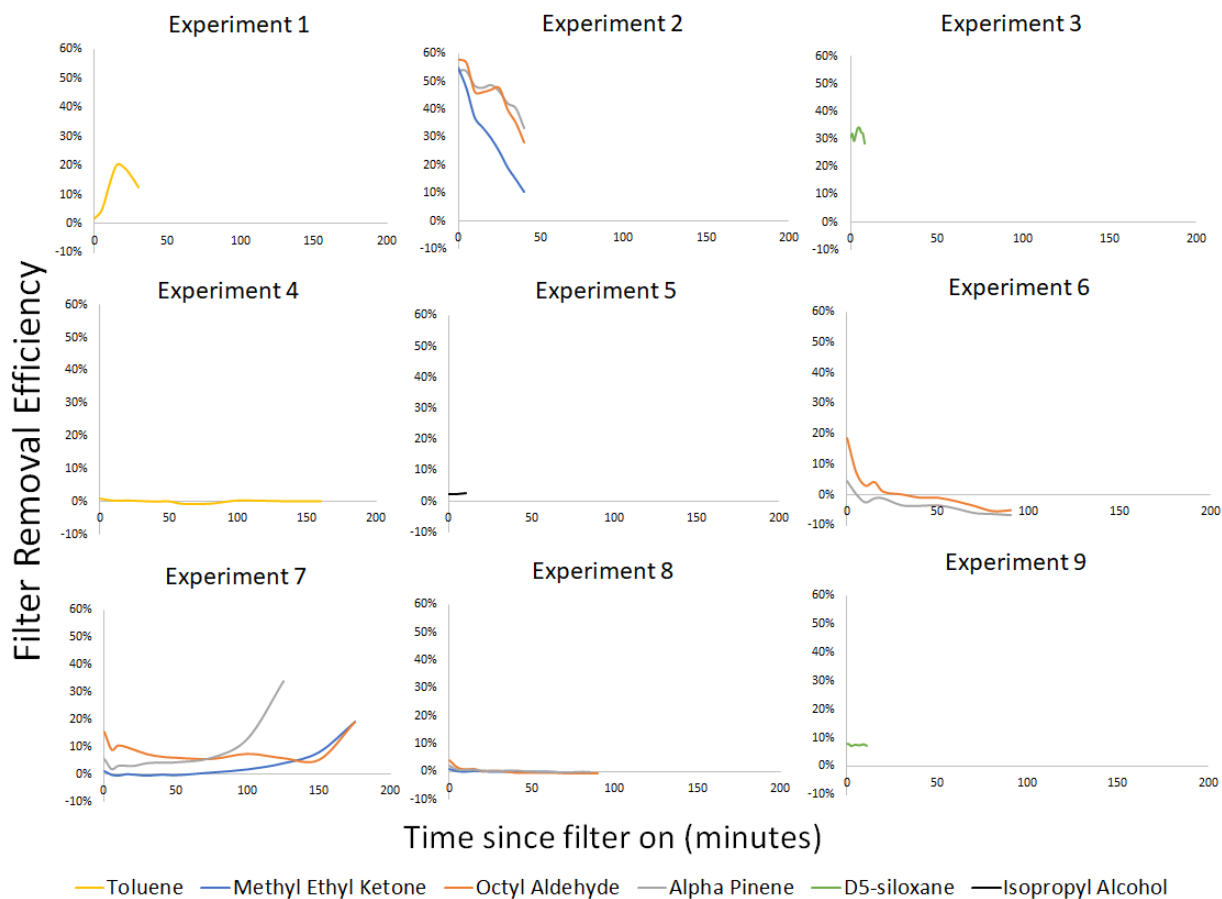


Figure 4.3: Summary of time-variant filter removal efficiencies for Experiments A1-A9. Generated using 5-minute period linear regressions

While filter flow rate is a parameter in the mass balance analysis, changes in residence time caused by filter flow rate changes may impact filter efficiency. The clearest test for the impact of filter flow rate is a comparison of experiments A6 and A8. However, filter removal efficiency in these tests was negligible, so no conclusions about the impact of filter flow rate can be drawn. The measured filter removal efficiencies from these experiments are listed in Table A1 in the appendix.

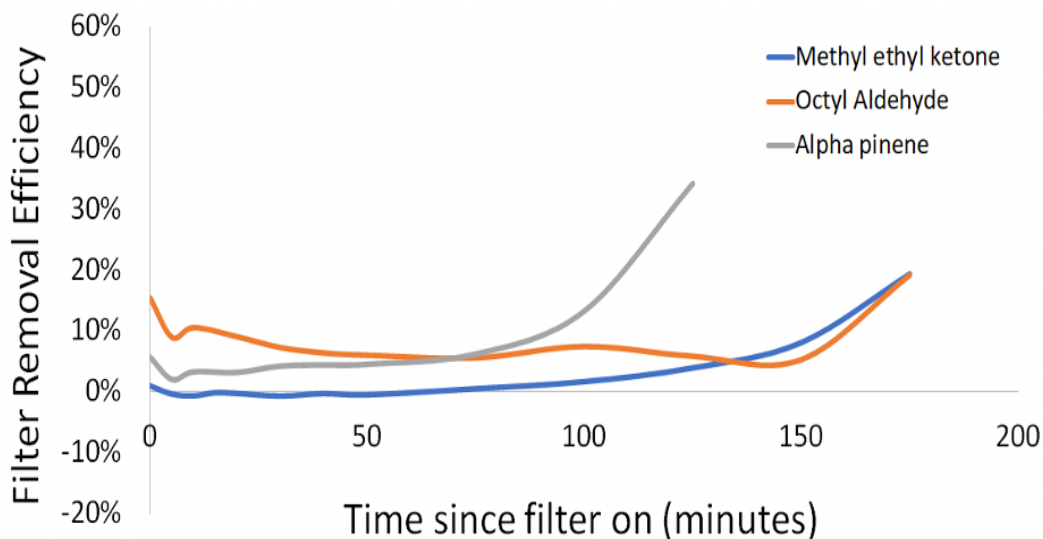


Figure 4.4: Time-variant 5-minute segmented filter efficiencies for Experiment A7

4.7 OFFGASSED COMPOUNDS FROM FILTER UNIT AND FILTER MEDIA

Prior to most decay experiments, filters were turned on in order to “degas” or desorb any compounds from the filter media. Experiments performed cannot distinguish between off-gassing from the filter unit itself and the filter media. The filter units were fairly new and had an obvious odor. Future experiments with older filter units should result in less impact from the filter unit itself. The offgassing of compounds may be dependent on the composition of filter holding trays including adhesives, plastics, and papers. Alternate material choices could significantly alter the profile of emissions.

Off-gassing emissions between activated carbon and photocatalyst tests did not vary dramatically. All tests included emission of toluene which is expected to be from adhesives used in filter tray construction. Additional compounds emitted included acrylic acid, propanamide, and toluene related compounds such as dehydrotoluene. In addition,

compounds which were previously injected in the chamber were not desorbed from filters in later experiments. There did not appear to be any dependence on previous injections on future desorption.

Chapter 5: Conclusions and Recommendations

5.1 CONCLUSIONS

In this study two phases of experiments were run. Phase 1 experiments served an exploratory purpose, illustrating experimental methods and data analysis techniques for calculating filter removal efficiency. Here volatile organic compounds including methyl ethyl ketone, toluene, α -pinene, octyl aldehyde, and D5-siloxane were tested using photocatalytic and activated carbon filters and filter removal efficiencies were calculated. Activated carbon filters had higher filter removal efficiencies than the photocatalytic oxidation filter operating at both 365 nm and 400 nm. The photocatalytic oxidation filter operated at 400 nm had higher filter removal efficiencies than when operated at 365 nm. The PCO filter operated at 365 nm had negligible removal efficiencies for methyl ethyl ketone, toluene, α -pinene, and octyl aldehyde, while the 400 nm PCO filter resulted in filter efficiencies higher than that of the 365 nm filter but significantly lower than the activated carbon filter.

Results from Phase 1 experiments influenced the choice to further test the filter removal efficiency of the PCO filter irradiated with 400 nm wavelength ultraviolet light. Phase 1 experiments had inconclusive results on the impact of filter flowrate on the filter efficiency hence the filter flowrate choice in phase 2 experiments was based on typical consumer use on the silent setting which is the lowest flowrate setting. The PCO filter when tested showed strong compound and pollutant concentration dependency in removal efficiency. Photocatalyst and activated carbon when used together improved filtration efficiency over photocatalyst alone. When compared to phase 1 experiments, activated carbon performed poorly in phase 2, potentially indicating some damage or loss of effectiveness in the activated carbon filter media. In general, this study suggests that photocatalytic technology may provide targeted utility for particular VOCs. Decay testing

of VOCs and products of bleach disinfection show low removal efficiencies for photocatalytic filters consistent with other studies involving the use of PCO filters in removing chlorinated species. Butyric acid and chloramine were removed at a higher efficiency, further indicating a possible compound specificity in photocatalytic reactions.

While the linear regression data analysis technique seemed to be appropriate for most experiments, non-linear behavior is observed. Data segmentation indicates how filter removal efficiency may be time dependent, both increasing, decreasing, and staying constant throughout an experiment. Decreases in filter efficiency may be related to filter saturation or poisoning, while increases in efficiency may indicate an inverse relationship between efficiency and concentration. Finally, off-gassing from filters did not seem to vary significantly based on filter type or previous compound exposure. This indicates that off-gassing from filter units is largely related to filter unit and filter tray construction.

5.2 RECOMMENDATIONS FOR FUTURE WORK

1. Moving forward, filter removal efficiency should be tested for different methods of filter deployment. Tests with a HVAC filter fitting should be carried out to better study the single pass efficiency of the filters when combined and used individually.
2. Effect of pollutant concentration should also be explored further. This study showed the possibility of a dependence on the pollutant concentration and this phenomenon should be studied further.
3. Filter efficiencies in removing chlorinated species should also be explored further. Taking into consideration the current need for regular disinfection of rooms in today's world and the adverse effect chlorinated species have

on human health, an understanding of the efficiency of air purifiers in removing these kinds of species will be valuable.

Chapter 6: Summary of Other Works

6.1 OBSERVING SEASONAL AIR QUALITY VARIATIONS FROM THE DELHI AEROSOL SUPERSITE (DAS) STUDY IN 2020

One of the world's most polluted megacities is New Delhi, India occasionally experiencing the highest particulate matter (PM) concentrations in the world (Gani et al., 2019). The seasons in Delhi are split into five, winter (December to mid-February), spring (mid-February to March), summer (April to June), monsoon (July to mid-September) and autumn (mid-September to November). Prior work by Gani et al., (2019) studies four seasons, winter, summer, monsoon and spring. Winter was observed to be the most polluted season and Monsoon was the least polluted. Organic PM₁ accounts for over 50% of all NR-PM₁ at all times of the day and in all seasons. Particulate matter levels were consistently higher in the cooler months and organic PM₁ were majorly from biomass burning in the cooler months (Gani et al., 2019). This summary highlights the observed non-refractory PM₁ (NR-PM₁) preliminary data from June 2020 – early November 2020 covering the summer, monsoon and most of the autumn season.

6.1.1 Materials and Methods

Measurements for the duration of this study were carried from a suite of online aerosol measurement instrumentation at the Indian Institute of Technology, Delhi (IITD) comprised of multiple instruments. An Aerosol Chemical Speciation Monitor (ACSM) was used to measure NR-PM₁, and particle size distributions (PSD) were occasionally measured using a Scanning Mobility Particle Sizer (SMPS). Data analysis carried out here is similar to that of Gani et al., (2019).

6.1.2 Overview of seasonal variations in 2020

An hourly averaged timeseries evolution of all NR-PM₁ species from June 2020 to early November 2020 is shown in figure 6.1. Concentrations are seen to gradually increase from summer to monsoon and a more rapid increase in autumn 2020 showcasing an increase from the warmer to cooler months.

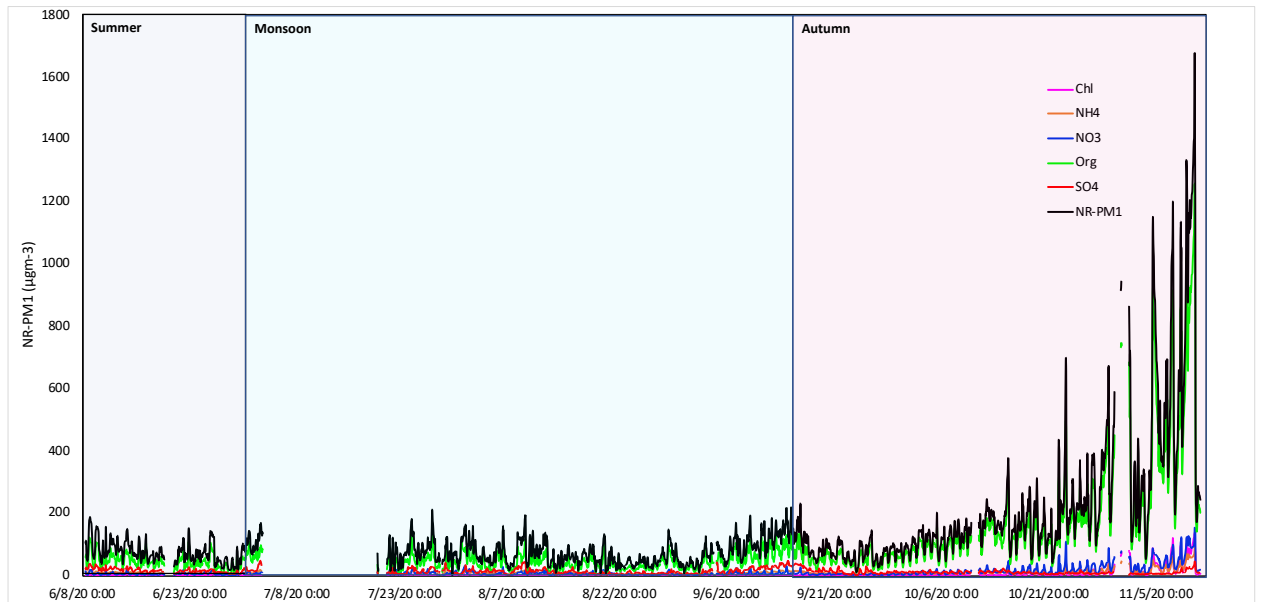


Figure 6.1: Timeseries of NR-PM₁ Species in from summer to fall 2020

Figure 6.2 shows the average seasonal composition of NR-PM₁ Species in 2020. As expected, organics have the highest contribution to the concentrations and chlorides have the lowest contribution across all seasons.

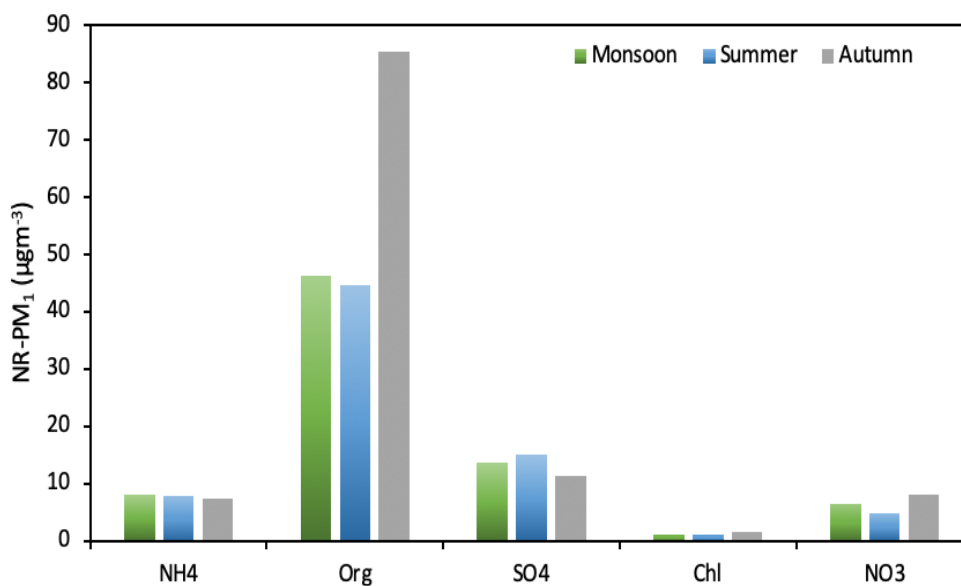


Figure 6.1: Average seasonal compositions of NR-PM₁ Species from 2020

Autumn season (Fall) has the highest total average NR-PM₁ concentrations as seen in figure 6.3. Fall being the coolest of all three seasons shown is expected to have the highest concentration and monsoon and summer have similar total concentrations however, monsoon has a higher concentration of nitrates.

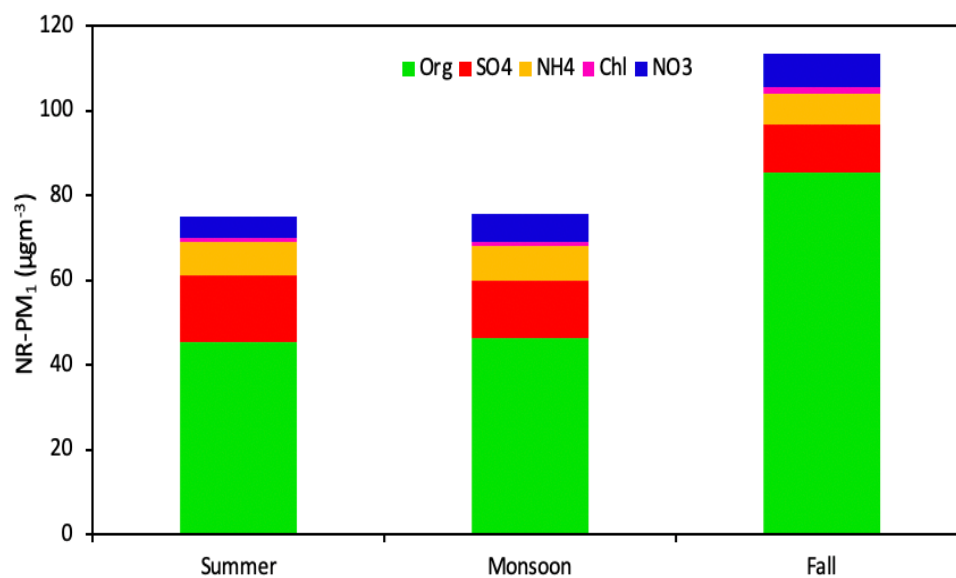


Figure 6.3: Average seasonal compositions of total NR-PM₁ from 2020

Figure 6.4 shows the fractional compositions of all the species across all three seasons. Organics have the highest fractional contribution of all the species across all three seasons and ammonium sulfates fractional contributions decrease significantly in fall.

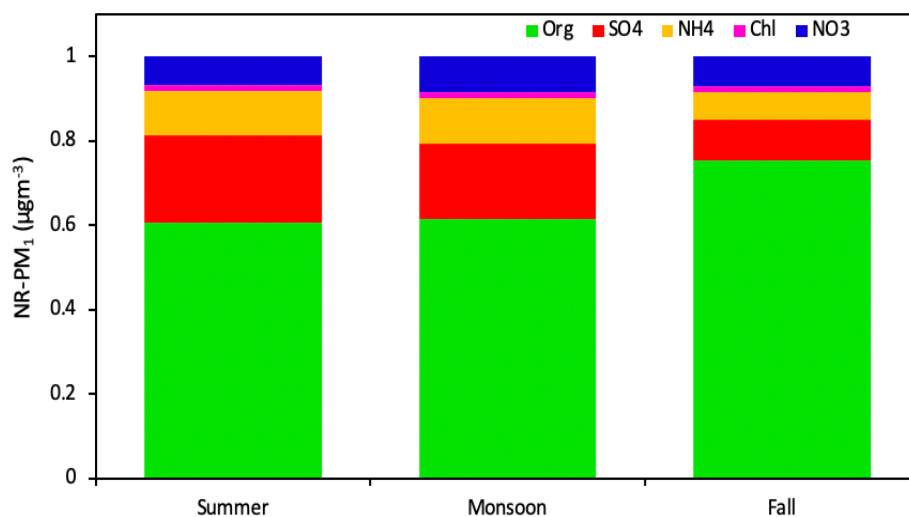


Figure 6.4: Fractional seasonal compositions of total NR-PM₁ from 2020

6.1.3 Diurnal variations across the seasons

Diurnal variations are observed across summer, monsoon and winter to establish if seasons have an observable effect on the diurnal trends of different species. Figure 6.5 shows that these trends remain consistent across all the seasons with an exception in ammonium in autumn. This difference occurs with a large peak at about 9:00 am at the same time we observe an increase in sulfates and a sharp decline in nitrates and chlorides. The trends with peaks in chlorides and nitrates, peak in sulfates and simultaneous decrease in ammonium is similar to observations from Gani et al., (2019).

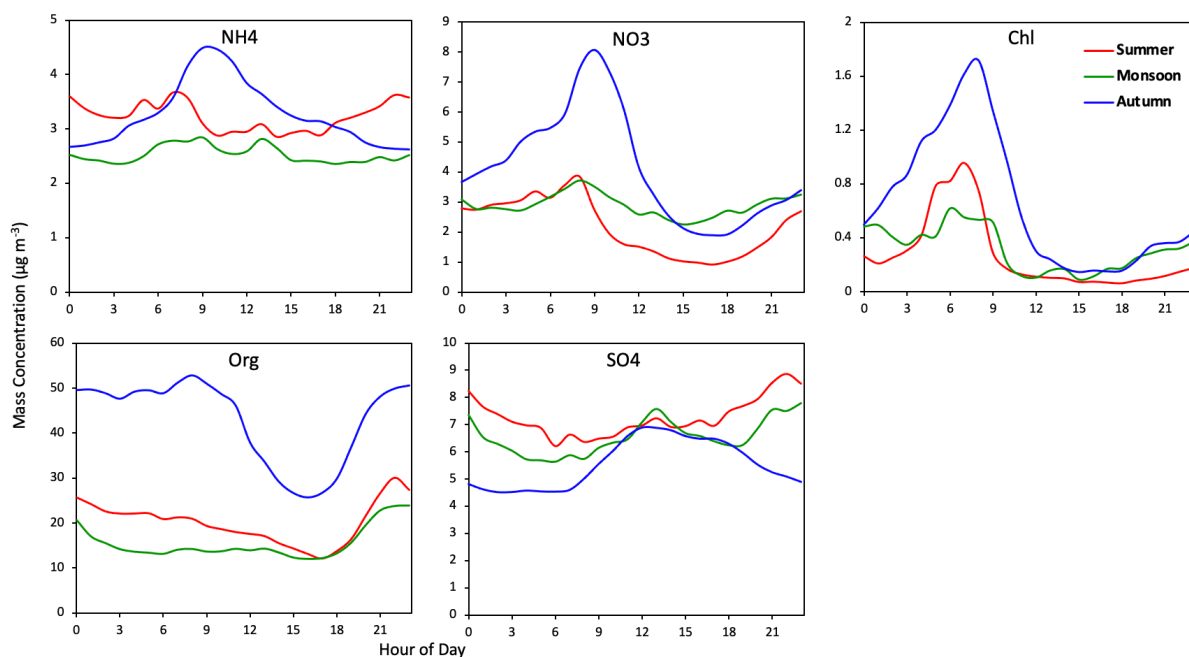


Figure 6.5: Average diurnal profiles of total NR-PM₁ from 2020

6.1.3 Conclusions and future work

Seasonal trends observed during summer, monsoon and fall seasons of 2020 are similar to the trends discussed in Gani et al., (2019). Cooler seasons have higher NR-PM₁ concentrations and warmer seasons have lower concentrations. Also, diurnal trends follow

similar patterns with an exception to ammonium. This difference should be looked at more closely.

Data shown in this summary is preliminary and still undergoing quality assurance which will be applied in future works. The data timeframe will be expanded to include the later months of 2020 and will be compared to data taken from earlier years.

Appendix

Table A1: Summary of experimental conditions and filter removal efficiencies from phase 1 experiments

Exp ID	Filter type	Layers	Wavelength (nm)	Filter flow rate (LPM)	Toluene	Methyl ethyl ketone	α -pinene	Octyl aldehyde	D5 siloxane	Isopropyl alcohol
A1	Activated Carbon	2	--	107	15%					
A2	Activated Carbon	2	--	25		30%	47%	45%		
A3	Activated Carbon	1	--	25					32%	
A4	Photocatalytic oxidation	2	365	107	0%					
A5	Photocatalytic oxidation	2	365	25						2.6%
A6	Photocatalytic oxidation	2	365	25			0%	0%		
A7	Photocatalytic oxidation	2	400	25		2.7%	14%	6.3%		
A8	Photocatalytic oxidation	2	365	107		0%	0%	0%		
A9	Photocatalytic oxidation	1	365	25					7.6%	
A10	Photocatalytic oxidation and Activated Carbon	2	365	25		5.5%	11%	0%		

Table A2: Summary of experimental conditions and filter removal efficiencies from phase 2 experiments^{c,d,e}

Exp ID	Species tested	Filter type	Layers	Methyl ethyl ketone	α -pinene	Butyric acid	Chlorine	Hypochlorous acid	Chloramine
B1	Bleach	Photocatalytic oxidation	1	--	--	--	< 5% ^a	--	--
B2	Bleach	Activated Carbon	1	--	--	--	< 5% ^a	LOD ^b	--
B3	Bleach	Photocatalytic oxidation & Activated Carbon	2	--	--	--	--	--	--
B4	VOC	Photocatalytic oxidation	1	8%	12%	37%	--	--	--
B5	VOC	Photocatalytic oxidation & Activated Carbon	2	12%	< 5% ^a	LOD ^b	--	--	--
B6	Bleach & VOC	Photocatalytic oxidation	1	--	--	--	--	--	--
B7	Bleach & VOC	Activated Carbon	1	--	--	--	--	--	--
B8	Bleach & VOC	Photocatalytic oxidation & Activated Carbon	2	22%	< 5% ^a	< 5% ^a	LOD ^b	LOD ^b	32%
B9	Bleach & VOC	Photocatalytic oxidation & Activated Carbon	2	7%	17%	42%	< 5% ^a	LOD ^b	LOD ^b
B10	Bleach & VOC	Photocatalytic oxidation & Activated Carbon	2	54%	73%	62%	LOD ^b	LOD ^b	17%

^a< 5% indicates that the removal efficiency value calculated was low. Values <5% are highly uncertain and cannot be quantified reliably.

^bLOD indicates that low measurement sensitivity and low concentrations make calculation of efficiency impossible

^cFilter flow rate for all experiments was maintained at 38 liters per second

^dWavelength used for all experiments was at 400nm

^eAir exchange rates were maintained at 0.97h⁻¹0.12

References

1. Zaatari, Marwa & Nirlo, Elena & Jareemit, Daranee & Crain, Neil & Srebric, Jelena & Siegel, Jeffrey. (2014). Ventilation and indoor air quality in retail stores: A critical review (RP-1596). HVAC&R Research. 20. 10.1080/10789669.2013.869126.
2. Chen, W., Zhang, J. S., & Zhang, Z. (2005). Performance of air cleaners for removing multiple volatile organic compounds in indoor air. *ASHRAE Transactions, 111 PART 1*, 1101–1114.
3. Chithra, V. S., & Shiva Nagendra, S. M. (2012). Indoor air quality investigations in a naturally ventilated school building located close to an urban roadway in Chennai, India. *Building and Environment*, 54, 159–167. <https://doi.org/10.1016/j.buildenv.2012.01.016>
4. Das, D., Gaur, V., & Verma, N. (2004). Removal of volatile organic compound by activated carbon fiber. *Carbon*, 42(14), 2949–2962. <https://doi.org/10.1016/j.carbon.2004.07.008>
5. Hedge, A. (2016). *Ergonomic Workplace Design for Health, Wellness, and Productivity*. CRC Press. <https://books.google.com/books?id=2RYNDgAAQBAJ>
6. Huang, Z. H., Kang, F., Liang, K. M., & Hao, J. (2003). Breakthrough of methylethylketone and benzene vapors in activated carbon fiber beds. *Journal of Hazardous Materials*, 98(1–3), 107–115. [https://doi.org/10.1016/S0304-3894\(02\)00284-4](https://doi.org/10.1016/S0304-3894(02)00284-4)
7. Luengas, A., Barona, A., Hort, C., Gallastegui, G., Platel, V., & Elias, A. (2015). A review of indoor air treatment technologies. *Reviews in Environmental Science and Biotechnology*, 14(3), 499–522. <https://doi.org/10.1007/s11157-015-9363-9>

8. Zhao, P., Siegel, J. A., & Corsi, R. L. (2007). Ozone removal by HVAC filters. *Atmospheric Environment*, 41(15), 3151–3160.
<https://doi.org/10.1016/j.atmosenv.2006.06.059>
9. Aktas, O. & Cecen, F. (2012) Fundamentals of Adsorption onto Activated Carbon in Water and Wastewater Treatment. ACTIVATED CARBON FOR WATER AND WASTEWATER TREATMENT: INTEGRATION OF ADSORPTION AND BIOLOGICAL TREATMENT.
10. U.S. Environmental Protection Agency. 1989. Report to Congress on indoor air quality: Volume 2. EPA/400/1-89/001C. Washington, DC.
11. U.S. Environmental Protection Agency. 1987. The total exposure assessment methodology (TEAM) study: Summary and analysis. EPA/600/6-87/002a. Washington, DC.
12. Wargoeki, P., Fanger, P.O., Krupicz, P. and Szczecinski, A. (2004) Sensory pollution loads in six office buildings and a department store, *Energy Build.*, 36, 995– 1001
13. Fang, L., Wyon, D.P., Clausen, G. and Fanger, P.O. 2002. Sick Building syndrome symptoms and performance in a field study at different levels of temperature and humidity, In: *Proceeding of Indoor Air 2002*, Monterey, California, USA. CD-ROM, The Printing House Inc., Stoughton, WI.
14. Skov, P. and Valbjorn, O. (1987) The sick building syndrome in office environment: the Danish Town Hall study, *Environ. Int.*, 13, 339–349.
15. Sundel, J., Lindvall, T. and Stenberg, B. 1991. Influence of type of ventilation and outdoor airflow rate on the prevalence of SBS symptoms. *Proceedings ofASHRAE Conference IAQ 1991*, Washington, DC, USA, pp 85–89.

16. Wargoeki, P., Wyon, D.P., Baik, Y.K., Clausen, G. and Fanger, P.O. (1999) Perceived air quality, Sick Building Syndrome (SBS) symptoms and productivity in an office with two different pollution loads, *Indoor Air*, 9, 165–179.
17. Bansal, R.C.R.C., Goyal, M., Roop, C.B., Meenakshi, G., Bansal, R.C.R.C., Goyal, M.: Activated Carbon Adsorption. Taylor & Francis Group (2005)
18. Haghghat, F., Lee, C.S., Pant, B., Bolourani, G., Lakdawala, N., Bastani, A.: Evaluation of various activated carbons for air cleaning—towards design of immune and sustainable buildings. *Atmos. Environ.* 42(35), 8176–8184 (2008)
19. Sidheswaran, M. A., Destailats, H., Sullivan, D. P., Cohn, S., & Fisk, W. J. (2012). Energy efficient indoor VOC air cleaning with activated carbon fiber (ACF) filters. *Building and Environment*, 47(1), 357–367. <https://doi.org/10.1016/j.buildenv.2011.07.002>
20. Hodgson, A. T., Destailats, H., Sullivan, D. P., & Fisk, W. J. (2007). Performance of ultraviolet photocatalytic oxidation for indoor air cleaning applications. *Indoor Air*, 17(4), 305–316. <https://doi.org/10.1111/j.1600-0668.2007.00479.x>
21. Sekiguchi, K., Ishitani, O., & Sakamoto, K. (n.d.). Removal of VOCs by Photocatalytic Degradation Involving Photochemical Reaction with O₃ Under Short-Wavelength UV Irradiation.
22. Krechmer, J., Lopez-Hilfiker, F., Koss, A., Hutterli, M., Stoermer, C., Deming, B., Kimmel, J., Warneke, C., Holzinger, R., Jayne, J., Worsnop, D., Fuhrer, K., Gonin, M., & de Gouw, J. (2018). Evaluation of a New Reagent-Ion Source and Focusing Ion-Molecule Reactor for Use in Proton-Transfer-Reaction Mass Spectrometry. *Analytical Chemistry*, 90(20), 12011–12018. <https://doi.org/10.1021/acs.analchem.8b02641>

23. Kim, S. B., Hwang, H. T., & Hong, S. C. (2002). Photocatalytic degradation of volatile organic compounds at the gas-solid interface of a TiO₂ photocatalyst. *Chemosphere*, 48(4), 437–444. [https://doi.org/10.1016/S0045-6535\(02\)00101-7](https://doi.org/10.1016/S0045-6535(02)00101-7)
24. Lee, B. H., Lopez-Hilfiker, F. D., Mohr, C., Kurtén, T., Worsnop, D. R., & Thornton, J. A. (2014). An iodide-adduct high-resolution time-of-flight chemical-ionization mass spectrometer: Application to atmospheric inorganic and organic compounds. *Environmental Science and Technology*, 48(11), 6309–6317. <https://doi.org/10.1021/es500362a>
25. Bhave, P. P., & Yeleswarapu, D. (2020). Removal of Indoor Air Pollutants Using Activated Carbon---A Review. In V. Sivasubramanian & S. Subramanian (Eds.), *Global Challenges in Energy and Environment* (pp. 65–75). Springer Singapore.
26. Mo, J., Zhang, Y., Xu, Q., Lamson, J. J., & Zhao, R. (2009). Photocatalytic purification of volatile organic compounds in indoor air: A literature review. *Atmospheric Environment*, 43(14), 2229–2246. <https://doi.org/10.1016/j.atmosenv.2009.01.034>
27. Wang, M., Chen, D., Xiao, M., Ye, Q., Stolzenburg, D., Hofbauer, V., Ye, P., Vogel, A. L., Mauldin, R. L., Amorim, A., Baccharini, A., Baumgartner, B., Brilke, S., Dada, L., Dias, A., Duplissy, J., Finkenzeller, H., Garmash, O., He, X. C., ... Donahue, N. M. (2020). Photo-oxidation of Aromatic Hydrocarbons Produces Low-Volatility Organic Compounds. *Environmental Science and Technology*, 54(13), 7911–7921. <https://doi.org/10.1021/acs.est.0c02100>
28. Ao, C. H., & Lee, S. C. (2004). Combination effect of activated carbon with TiO₂ for the photodegradation of binary pollutants at typical indoor air level. *Journal of Photochemistry and Photobiology A: Chemistry*, 161(2–3), 131–140. [https://doi.org/10.1016/S1010-6030\(03\)00276-4](https://doi.org/10.1016/S1010-6030(03)00276-4)

29. Gallego, E., Roca, F. J., Perales, J. F., & Guardino, X. (2013). Experimental evaluation of VOC removal efficiency of a coconut shell activated carbon filter for indoor air quality enhancement. *Building and Environment*, 67, 14–25. <https://doi.org/10.1016/j.buildenv.2013.05.003>
30. Xingzhou, H. (1997). *Wavelength sensitivity of photo-oxidation of polyethylene*. *Polymer Degradation and Stability*, 55(2), 131–134. [https://doi.org/10.1016/s0141-3910\(96\)00120-6](https://doi.org/10.1016/s0141-3910(96)00120-6)
31. Zhang, Z., Hu, X., & Luo, Z. (1996). *Wavelength sensitivity of photooxidation of polypropylene*. *Polymer Degradation and Stability*, 51(1), 93–97. [https://doi.org/10.1016/0141-3910\(95\)00210-3](https://doi.org/10.1016/0141-3910(95)00210-3)
32. Driessen, M. D., & Grassian, V. H. (1998). *Photooxidation of trichloroethylene on Pt/TiO₂*. *Journal of Physical Chemistry B*, 102(8), 1418–1423. <https://doi.org/10.1021/jp9724075>
33. Gani, S., Bhandari, S., Seraj, S., Wang, D. S., Patel, K., Soni, P., & Arub, Z. (2019). *Submicron aerosol composition in the world's most polluted megacity: the Delhi Aerosol Supersite study*. 5, 6843–6859.